Application of Hyperion hyperspectral imagery on geological mapping in Central Mountain Range of Taiwan: preliminary results

W.-S. Chang
Department of Earth Sciences, National Cheng Kung University
No 1, Ta-Hsueh Road, Tainan 701, China Taipei
l4693406@mail.ncku.edu.tw

C.-C. Liu
Department of Earth Sciences, National Cheng Kung University
No 1, Ta-Hsueh Road, Tainan 701, China Taipei
ccliu88@mail.ncku.edu.tw

Abstract: The characteristics of geological material, such as the lithology and mineral composition, provide important information in geohazard assessment and mineral exploration. The lofty Central Mountain Range located in the mid east of Taiwan was formed by the slow collision of the Asian continental plate and the Philippine plate, resulting in a 340-km x 80-km area with average height of 2000-m where implementation of the traditional approach of geological survey is impractical. Up to now, very little is known about the characteristics of geological material in this area. The hyperspectral imagery obtained from the airborne platform had been applied in lithology mapping since 1980s. All ideal results were reported in the sparse-vegetation and well-exposed outcrop area. The space-borne Hyperion sensor onboarded the EO-1 satellite was successful deployed in November 2000. Its advanced spectral range and resolution motivates us to apply the hyperspectral imagery to the work of geological mapping in the Central Mountain Range of Taiwan. The challenge is that the coverage of vegetation is dense while the useful outcrop is relatively sparse in this area.

To apply the hyperspectral imagery to the work of geological mapping in dense-vegetation and sparse-outcrop region, we investigate the feasibility by conducting a numerical experiment with simulated hyperspectral imagery. The spectra of different surface features are selected and mixed under various controlled conditions. A series of hyperspectral unmixing processing was taken and the results were compared to the simulated conditions. Even though the outcrop area is too small to constitute a pure pixel, results from this experiment indicate that the outcrop still can be identified, as long as the spectra of that particular outcrop is measured and provided as an endmember in the processing. We took a further step to process and analyze the Hyperion image taken on 5 June 2005 in this area. The commercial package, FLAASH 4.1, was employed to correct the atmospheric effect. The ground truths were collected during several field works to the Pao-Lai and He-Ping sites. Various samples of rocks were brought back to the lab to measure the spectral reflectance using a hyperspectral spectroradiometer (GER 2600). These spectra were supplied as endmembers in the processing of Hyperion image. The standard approaches of mixed-pixel analysis were followed and the results of classification were compared to the existing geological map. Results of this research encourage the application of Hyperion hyperspectral imagery on geological mapping in Central Mountain Range of Taiwan.

Keyword: hyperspectral, Hyperion, geological mapping

1. Introduction

The characteristics of geological material, such as the lithology and mineral composition, provide important information in geohazard assessment and mineral exploration. The lofty Central Mountain Range (CMR) of Taiwan was formed by the slow collision of the Asian continental plate and the Philippine plate. A comprehensive explorations of the geological composition have been made in the middle-low elevation above sea level of Taiwan [1], where the regions are accessible and the traditional approach of geological survey can be conducted. For those areas with average height of 2000-m and above, however, the implementation of the traditional approach of geological survey is impractical. Therefore, the report of the geological material and characteristics in this region is limited. In order to acquire more geological material information for geohazard assessment and mineral exploration, a practical approach of geological survey in the CMR of Taiwan is urgently needed [2].

Various minerals or rocks have different spectral characteristics in the spectral range from 400 to 2500 nm. By detecting the subtle differences of these spectral characteristics, especially in the short-wavelength infrared (SWIR) ranged from 2000 to 2500 nm [3, 4], the airborne hyperspectral imagery has been successfully applied to lithology mapping since 1980s [4]. Up to now, however, all ideal results of lithology mapping were reported in the well-exposed area with sparse covers of vegetation, such as the work of Rowan [5] and Kruse [4]. The space-borne Hyperion sensor onboarded the EO-1 satellite was successful deployed in November 2000. Hyperion data is recorded in 242 bands from 356 to 2578 nm with approximately 10-nm spectral resolution and 30-m spatial resolution. With the advantages of taking synoptic view of the broad area from the space-borne platform, the Hyperion hyperspectral imagery might provide an avenue to map the geological composition in the CMR of Taiwan. The challenge is that the coverage of vegetation is dense while the useful outcrop is relatively sparse in this area.

This paper reports the preliminary results of lithologic mapping in the CMR of Taiwan using the Hyperion hyperspectral imagery taken on June 5, 2005. Because the typical climate in the CMR of Taiwan is both humid and warm, most of the study areas are covered by vegetation, except for a few outcrops distributed sparsely. We employed a mask to delineate the outcrop regions from the Hyperion imagery. Two field trips were conducted to collect the samples of rocks in several outcrop areas. The reflective spectra of these samples were carefully measured in the lab using the spectroradiometer GER 2600 under the ideal conditions of natural illumination. These spectra were served as another source of endmembers in the processing of hyperspectral imagery. To correct the atmospheric effects, we employed the commercially available package, FLAASH 4.1, to retrieve the surface reflectance. The results of atmospheric correction were evaluated by comparing to the known reflective spectra in some outcrop areas. Following the procedures described in Kruse [4], we conducted a series of processing to identify the pure pixels, extract the spectra of endmembers, and unmix each pixel to estimate the lithological composition of each pixel. The preliminary results of this research shows that the lithology of the study area comprises of low to high-grade metamorphic rocks, such as argillite and slate of Lushan and Pilushan Formation, metamorphic limestone (marble) and schist of Tananao Schist. Comparing our results to the 1:500,000 scale geological map [6] shows that a reasonable classification of lithological composition can be obtained from the Hyperion imagery. Results of this research encourage the application of Hyperion hyperspectral imagery on geological mapping in CMR of Taiwan.

2. Study Area

The study area locates in the mid east of Taiwan with approximately 7.5 km in width and 86 km in length (Fig. 1), including Yilan, Hualian, Taichung, and Nantou County. This area was formed by the slow collision of the Asian continental plate and the Philippine plate. Since the average height of this area is more than 2000-m, the implementation of the traditional approach of geological survey is impractical. Although the heavy slips of the precipitous hillsides prohibits the possibility of any train running or highway constructed in this area, a few pathways are still laid out in part of this area to transport timbers. This gives some information of the transections in this area. Two field works to this area were conducted to collect samples of rocks from the outcrops in the Pao-Lai and He-Ping sites, respectively. The triangle symbol in Fig. 1 represents the locations where the samples were taken.

One important source of the geological map was published by the Central Geological Survey of Taiwan in 2000 with 1:500,000 scale [6]. This map categozies the lithology of the study area into three major formations, including (1) the Miocene argillite, slate and phyllite that are low-grade metamorphic rocks of Lushan Formation underlaid one-third of the northwest of the study area; (2) the higher-grade metamorphic Eocene slate and phyllite of Pilushan Formation in the central part of the study area; and (3) the schist and metamorphic limestone that are middle to high-grade metamorphic rocks (Tananao Schist) underlaid one-third of the southeast of the study area (Fig. 2). The weather in Taiwan is both humid and warm all year around. Consequently, most of the study areas are covered by vegetation, except for a few outcrops distributed sparsely.

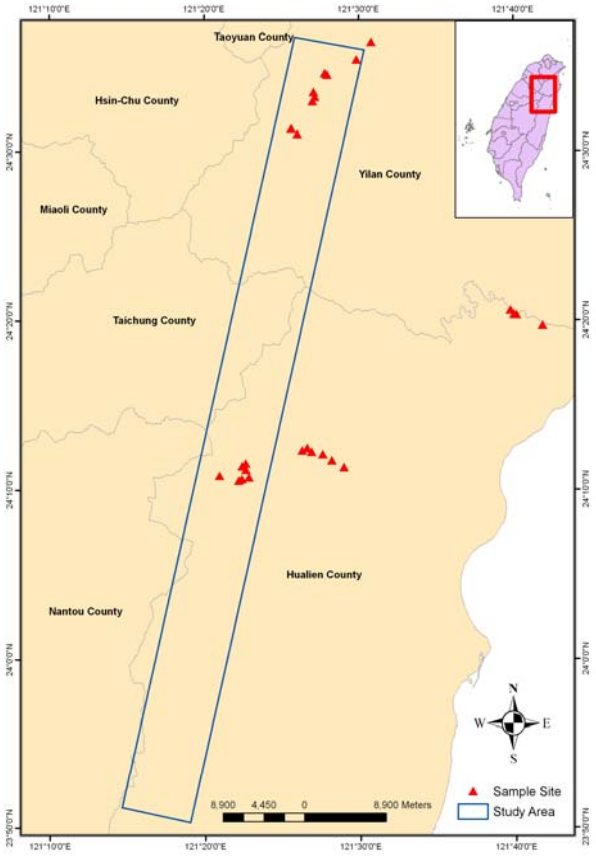

Fig 1. Study area and sample sites.

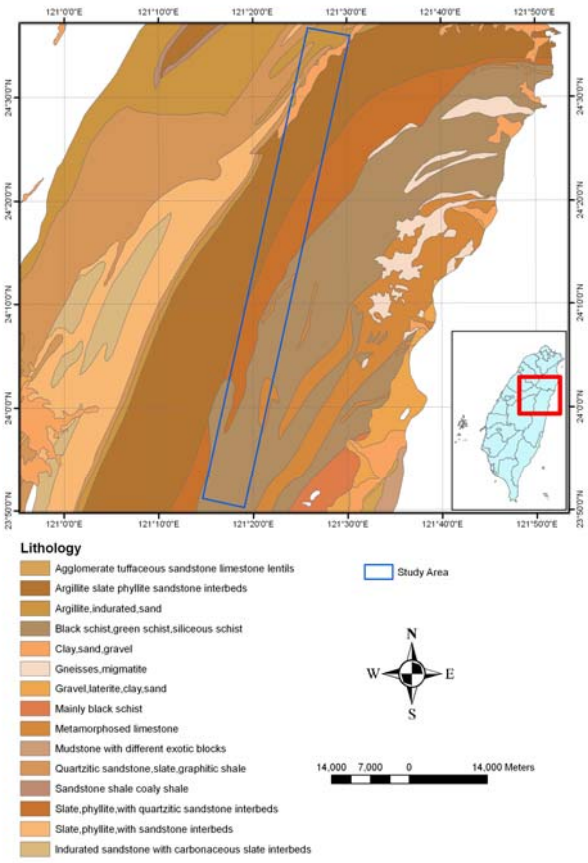

Fig 2. 1:500,000 scale geological map

3. Data

1) Sample spectra

The spectral libraries of various minerals and rocks had been investigated and compiled in the past by several research institutes, such as USGS, NASA-JPL and John Hopkins University. However, our earlier work [7] indicates that the existing spectral libraries are not fully comparable to the *in situ* measurements of reflectance, especially for some soils and rocks in Taiwan area. In order to establish a reliable base of spectral library, we collected a considerable amount of samples in the aforementioned two field trips, which include gneiss, dolomite, black schist, green schist, marble, slate, black slate and amphibolite, as denoted in the legend of Fig. 1. These samples were brought back to the lab and the hyperspectral spectroradiometer (GER 2600) was used to measure the spectral reflectance of each sample. The spectral range of the GER 2600 spectroradiometer is from 350 to 2500 nm with different bandwidths at different wavelengths: 1.5 nm in 350—1050 nm and 11.5 nm in 1050—2500 nm. The measured spectra of all samples are shown in Fig. 3(a).

Since the shortwave infrared (SWIR) spectral range (2000—2500 nm) covers several important spectral features of minerals, the SWIR range in Fig 3(a) is further enlarged in Fig 3(b) for examination. At least five spectral features can be verfied by inspecting Fig 3(b): (1) the spectra of dolomite and marble exhibit CO_3 absorption feature centered at 2314 nm and 2335 nm, respectively [3, 5, 8]; (2) the spectrum of gneiss shows the absorption features at 2254, 2324 and 2355 nm that are mainly due to Fe, Mg-OH in amphibole and biotite [8]; (3) the spectrum of amphibolite composed mainly by amphiboles indicate Fe, Mg-OH absorption feature located at 2304 and 2324 nm [8]; (4) Both the spectra of black schist and green schist illustrate the differences between the biotite-dominant spectrum and the chlorite and epidote-dominant spectrum, as well as theirs absorption features centered at 2324 and 2355 nm, respectively [8]. These spectra serve as a reliable base of endmembers for further analysis of Hyperion hyperspectral imagery.

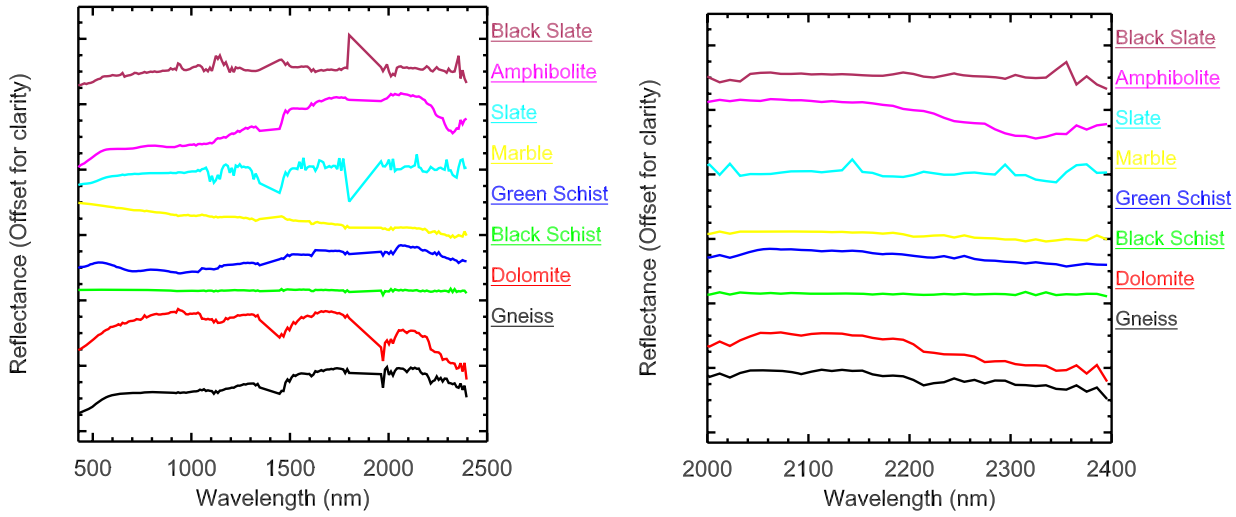

Fig 3. Reflectance spectra of rock sample. Reflectance spectra were resampled to Hyperion bands (left). Reflectance spectra in the SWIR region have more spectral feature of minerals (right) [3, 4].

2) Hyperion image

The first space-borne hyperspectral sensor, Hyperion onboarded the EO-1 satellite, was successful deployed in a near-polar orbit in November 2000. Hyperion is a pushbroom instrument covering the spectral range from 356 to 2578 nm with 242 spectral bands but only 198 bands are calibrated. Because of an overlap between the VNIR and SWIR focal planes, there are only 196 unique channels [9]. Note the spectra of samples as shown in Fig. 3 were also resampled to these 196 bands in the following processing. Its spectral resolution is approximately 10-nm and spatial resolution is about 30-m. Since there was no any image of the study area in the existing database of Hyperion imagery, we placed an order to take one Hyperion image over the study area on May 4, 2005. Due to the high coverage of cloud taken on that day, two images of the same area were taken on May 20 and June 5, respectively. Fig. 5(a) shows the full scene of the image taken on June 5, 2005, which has the lowest cloud coverage (29%) among the three images. To avoid the analysis of those areas covered by clouds, only the middle part of the original Hyperion image was selected and enlarged in Fig. 5(b) for further processing.

4. Methods

Kruse et al. [4] gave a detailed description of the hyperspectral image analysis that is implemented in ENVI image processing software. We followed the same approach except for using the commercial package, FLAASH (Fast Line-of-sight Atmospheric Analysis of Spectral Hypercubes) 4.1 [10], to correct the atmospheric effect. The analysis is briefed as follows:

1) Atmospheric Correction

To retrieve the surface reflectance from the at-sensor radiance measured by Hyperion, the atmospheric effect needs to be corrected with special care. The FLAASH was developed by Spectral Sciences, Inc. in collaboration with U.S. Air Force Research Laboratory (AFRL). It is profited from the very latest MODTRAN radiation transfer code that is able to consider the atmospheric water vapor, oxygen, carbon dioxide, methane, ozone, and molecular and aerosol scattering [10]. To evaluate the results of atmospheric correction using FLAASH, the spectrum of the sample taken at a known site is compared to the before- and after- FLAASH corrected spectra (Fig. 4). This site is abundant of marble that exhibits the CO_3 absorption feature at 2314 nm and other absorption features at 2203 nm, 2234 nm, 2324 nm, 2355 nm, and 2385 nm. The original Hyperion image gives a smooth spectrum that lacks most of the features. Although the actual values of spectra are not exactly the same between the sample and the atmospheric-corrected image, all of the absorption features are indeed shown in the atmospheric-corrected spectra. This is crucial for hyperspectral analysis, especially using the approach of Spectral Angle Mapper (SAM) that only considers the band ratio rather than the actual values.

2) Hyperspectral Analysis

As aforementioned, the SWIR spectral range (2000—2500 nm) covers several important spectral features of

minerals, we focus on this range of which the Hyperion has a total of 40 bands. Kruse [4] pointed out that the Hyperion image is suffered from the low signal-to-noise ratio. The apparent strips are frequently found in several bands. To reduce the errors caused by the stripping effect, we screened all spectral bands and manually rejected a total of 18 bands with apparent stripping effects from SWIR spectral range. As a result, the Hyperion image as shown in Fig. 5(b) was reduced to 22 bands for further processing.

In order to avoid the interference from the dense vegetation and get clear signals from the area of outcrop, we applied a mask to the atmospheric-corrected Hyperion image and delineate the outcrop regions (Fig. 5C). The following procedures of hyperspectral analysis were employed, including the Minimum Noise Fraction (MNF) transformation for reducing spectral data, the Pixel Purity Index (PPI) for identifying those extreme or spectrally pure pixels, and the n-Dimensional Visualizer for determining the endmembers directly from the image [4, 5, 8]. The approach of SAM was then employed to identify the rock type of those endmembers retrieved from the image [5]. Finally, the Mixture-Tuned Matched Filtering (MTMF) was used for lithologic mapping [4].

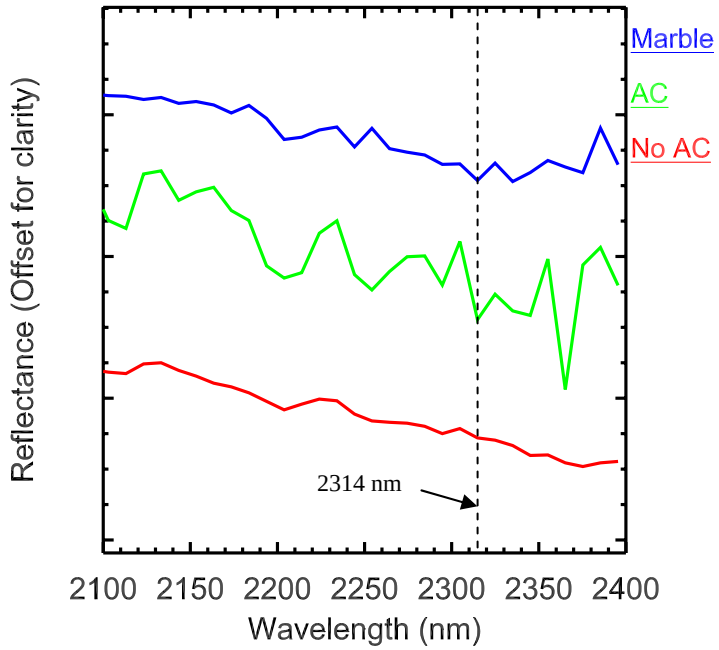

Fig 4. The reflectance spectra of the test site before and after atmospheric correction and a marble spectrum collected using hyperspectral spectroradiometer (GER 2600).

5. Result and Discussion

22 bands covering the shortwave infrared spectral range were linearly transformed using MNF transformation. The MNF result indicates that the dimensionality is approximately seven. The top seven MNF bands contain most of the spectral information [4]. Therefore, they were used to determine the pure pixels in the Hyperion image using PPI procedure. The spectra of pure pixels were plot into an n-dimensional scatterplot to determine the pure pixels with endmembers. These endmembers than to be identified using SAM procedure and those sample spectra measured in the lab using the spectroradiometer GER 2600 resampled to 22 bands were used as referent spectra in spectral analyst. There are five endmembers were been identified as black schist, black slate, amphibolite, marble, and green schist in this research. Once a series of extracting and identifying endmembers were completed, and those endmembers were

used for classification. In order to make a lithologic map, MTMF which is a spectral matching method was to use. The result of MTMF is the distribution and the abundance of selected endmembers [4], and a lithologic map was been generated from thresholded MTMF products. The Fig. 5D shows the lithologic map includes five rock types, and the threshold of MTMF products is 0.5.

We selected six regions having more and larger outcrops from study area (Fig. 5C) to make a detail discussion about MTMF products of five rock types including black schist, black slate, amphibolite, marble, and green schist (Fig. 6). The formation of these six regions is described in below: region one and two located in Lushan Formation; region three located in Pilushan Formation; region four located both in Pilushan Formation and Tananao Schist; region five and six located in Tananao Schist. Visual comparison of those MTMF products of five rock types shows that distribution of black schist and black slate is approximately the same and evenly distributes six regions. The different between black schist and black slate is abundance. There is more black schist in these six regions. Note the distribution of amphibolite concentrates in the region five and six and the abundance here is extremely high. And the MTMF product of marble shows that marble distributes all of the six regions and mainly concentrate in the region one and two with high abundance. As for green schist, the distribution is over the six regions and having higher abundance in the region five and six.

Results of MTMF procedure were compared to the 1:500,000 scale geological map and the results are as follows, the distribution of black schist, black slate and green schist conforms to the geological map. All of the three formations in the study area possibly include black schist and black slate. Green schist may exist in the three formations and more probably in Tananao Schist which contains higher-grade metamorphism such as green schist. Therefore, the green schist majority of distributions in the region five and region six are reasonable. Analysis result suspicious occupying in marble distribution. According to geological map demonstration marble distribution should in the region six, nevertheless, the marble mainly distributes in the region one and two in this research. The reason for this phenomenon is possibly the spectral range of image to analyzing did not cover marble characteristic wavelength which located at 2335nm. And another possibly reason is the spectrum of marble sample has problem due to atmospheric condition or operation mistake by human while measuring. In the case of amphibolite, the 1:500,000 scale geological map does not illustrate the amphibolite rock type in the study area. For this reason, we have not discussed the accuracy of amphibolite in this research.

6. Conclusion

Comparing our results to the 1:500,000 scale geological map shows that a reasonable classification of lithological composition can be obtained from the Hyperion SWIR spectrometer (2000—2400 nm). Lithologies mapped in this study area include black schist, black slate, amphibolite, marble, and green schist. Most of these rocks distribution are reasonable expect marble probably due to spectral range for analyzing didn’t cover marble characteristic wavelength or some wrong in marble reference spectrum.

The limits of the Hyperion imagery for lithological mapping are the apparent strips in several bands even those important absorption bands and the low signal-to-noise ratio of imagery. To improve the accuracy of lithological mapping, we should collect more precise spectra of samples. Results of this research encourage the application of Hyperion hyperspectral imagery on geological mapping in CMR of Taiwan.

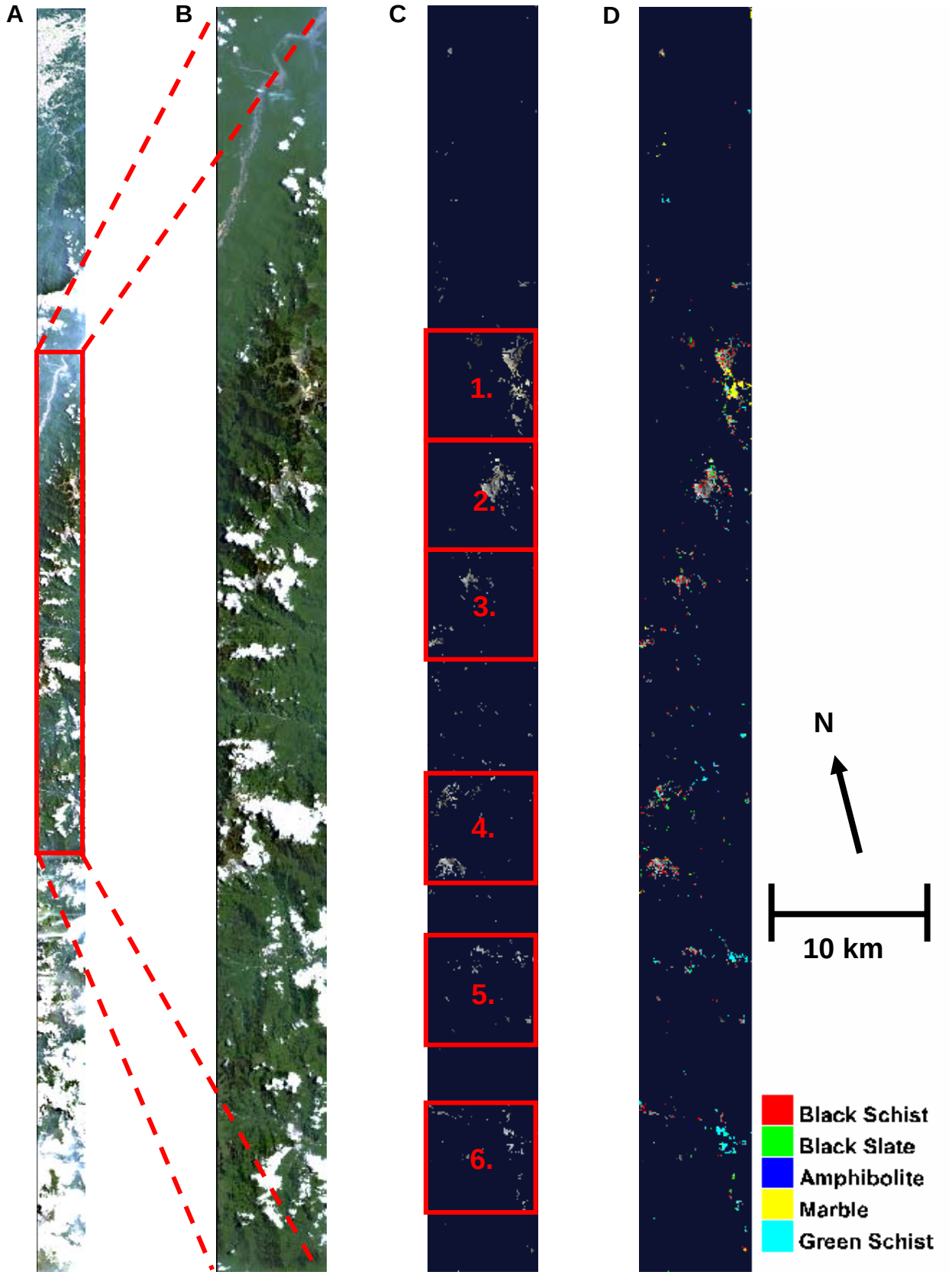

Fig 5. The true color composite (red: 640.5 nm; green: 548.92 nm; blue: 457.34 nm) of (A) the orginal Hyperion image acquired on June 5, 2005 with 29% cloud coverage, (B) the center part of the original imagery with lower cloud cover (7.5 km in width and 86 km in length), and (C) the outcrops after applying the cloud and vegetation masks. The results of MTMF analysis for all corresponding outcrops are shown in (D).

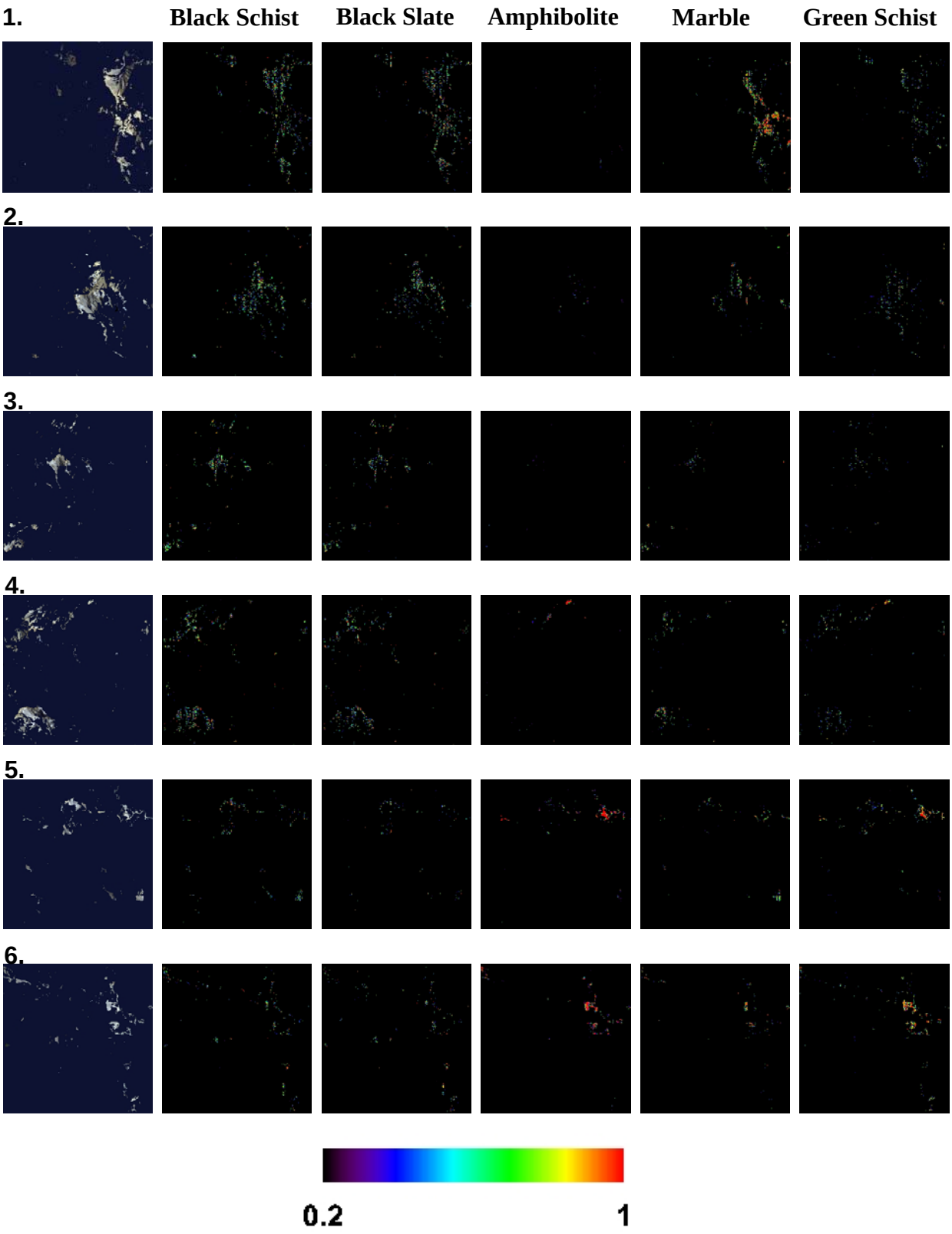

Fig 6. Results of MTMF analysis in six selected regions as denoted as red boxes in Fig. 5C, including black schist, black slate, amphibolite, marble, and green schist.

Acknowledgement

We thank Dr. Chwen-Ming Yang for providing the assistance in using the GER2600 spectroradiometer. This research was supported by the National Science Council of Taiwan through grants NSC 93-2625-Z-006-011, and the Central Geology Survey of Taiwan through grants 5226902000-07-94-01.

References

[1] Central Geological Survey, MOEA, 2002, Geological data conformity inquiry system, *http://210.69.81.69/geo/begin_internet.cfm*.

[2] C.-C. Lin, K.-S. Shea, C. Hua-Wen, M.-M. Chen, S.-F. Chang, C.-W. Lin, C.-C. Liu, and C.-L. Shieh, 2005, A dynamic system for monitoring the geologic environment and geohazard in Taiwan by using FORMOSAT-2 images, *2005 Annual Meeting of Geological Society*.

[3] R. P. Gupta, 2003, *Remote Sensing Geology*.

[4] F. A. Kruse, J. W. Boardman, and J. F. Huntington, 2003, Comparison of Airborne Hyperspectral Data and EO-1 Hyperion for Mineral Mapping, *IEEE Transactions on Geoscience and Remote Sensing*, vol. 41, 1388-1400.

[5] L. C. Rowan and J. C. Mars, 2003, Lithologic mapping in the Mountain Pass, California area using Advanced Spaceborne Thermal Emission and Reflection Radiometer (ASTER) data, *Remote Sensing of Environment*, vol. 84, 350-366.

[6] Central Geological Survey, MOEA, 2000, Geologic map of Taiwan (1:500,000).

[7] C.-C. Liu, W.-S. Chang, C.-W. Lin, C.-M. Yang, J.-G. Liu, and C.-L. Shieh, 2005, In situ measurement, interpretation and application of the hyperspectral reflectance of laterite in Linkuo plateau, *2005 Annual Meeting of Geological Society*.

[8] L. C. Rowan, C. J. Simpson, and J. C. Mars, 2004, Hyperspectral analysis of the ultramafic complex and adjacent lithologies at Mordor, NT, Australia, *Remote Sensing of Environment*, vol. 91, 419-431.

[9] R. Beck, 2003, *EO-1 User Guide v. 2.3*.

[10] Research Systems, Inc, 2001, *FLAASH User's Guide*.